The Astrophysical Journal, 600:986–991, 2004 January 10

PROCESSING OF PRESOLAR GRAINS AROUND POST–ASYMPTOTIC GIANT BRANCH STARS: SILICON CARBIDE AS THE CARRIER OF THE 21 MICRON FEATURE

Angela K. Speck
Physics and Astronomy Department, University of Missouri, Columbia, MO 65211; speckan@missouri.edu

and

Anne M. Hofmeister
Department of Earth and Planetary Science, Washington University, Box 1169, 1 Brookings Drive, St. Louis, MO 63130
Received 2003 July 7; accepted 2003 September 25

ABSTRACT

Some proto–planetary nebulae (PPNs) exhibit an enigmatic feature in their infrared spectra at ~21 μm. This feature is not seen in the spectra of either the precursors to PPNs, the asymptotic giant branch (AGB) stars, or the successors of PPNs, "normal" planetary nebulae (PNs). However, the 21 μm feature has been seen in the spectra of PNs with Wolf-Rayet central stars. Therefore, the carrier of this feature is unlikely to be a transient species that only exists in the PPN phase. This feature has been attributed to various molecular and solid-state species, none of which satisfy all constraints, although titanium carbide (TiC) and polycyclic aromatic hydrocarbons (PAHs) have seemed the most viable. We present new laboratory data for silicon carbide (SiC) and show that it has a spectral feature that is a good candidate for the carrier of the 21 μm feature. The SiC spectral feature appears at approximately the same wavelength (depending on the polytype/grain size) and has the same asymmetric profile as the observed astronomical feature. We suggest that processing and cooling of the SiC grains known to exist around carbon-rich AGB stars are responsible for the emergence of the enigmatic 21 μm feature. The emergence of this feature in the spectra of post-AGB stars demonstrates the processing of dust due to the changing physical environments around evolving stars.

Subject headings: astrochemistry — circumstellar matter — methods: laboratory — stars: AGB and post-AGB — stars: mass loss — stars: winds, outflows

1. INTRODUCTION

Intermediate-mass stars (0.8–8.0 $M_{\odot}$) eventually evolve on the Hertzsprung-Russell diagram, up the asymptotic giant branch (AGB; Iben & Renzini 1983). The intensive mass loss that characterizes the AGB produces a circumstellar shell of dust and neutral gas. At the end of the AGB, mass loss virtually stops, and the circumstellar shell begins to drift away from the star. At the same time, the central star begins to shrink and heat up from ~3000 K until it is hot enough to ionize the surrounding gas, at which point the object becomes a planetary nebula (PN). The short-lived post-AGB phase, as the star evolves toward to the PN phase, is also known as the proto–planetary nebula (PPN) phase. A fast wind develops at some point during the PPN phase, which has very high velocities (~1000 km s^{-1}) and low mass. The detached dust shell drifting away from the central stars causes the PPN to have cool infrared colors from the cooling dust shell, but the decreasing optical depth of the dust shell as it expands allows the central star to be seen, making these objects optically bright.

PPNs can have either oxygen (O)- or carbon (C)-rich chemistries that control the nature of the dust in these objects. The chemistry depends on the prior chemical evolution of the progenitor AGB star. Among the C-rich PPNs, approximately half exhibit a feature in their infrared spectra at ~21 μm (Omont et al. 1995). Subsequent higher resolution data revised the so-called 21 μm position to 20.1 μm (Volk, Kwok, & Hrivnak 1999). PPNs that display this feature are all C-rich and all show evidence of *s*-process enhancements in their photospheres, indicative of efficient dredge-up during the ascent of AGB (Van Winckel & Reyniers 2000). This feature is not seen in the spectra of either the PPN precursors, AGB stars, or in their successors, PNs. A tentative observation of the 21 μm feature in PNs with Wolf-Rayet central stars was presented by Hony, Waters, & Tielens (2001) (see also Volk et al. 2003); however, there is some question as to whether these features are artifacts induced during spectral subtraction of the continuum (see Cohen et al. 2002). If these apparent features are indeed real, then the carrier can survive into the PN phase. In addition, the observed peak positions and profile shapes of the 21 μm feature are remarkably constant (Volk et al. 1999).

This enigmatic feature has been widely discussed since its discovery (Kwok, Volk, & Hrivnak 1989) and has been attributed to a variety of both transient molecular and solid-state species (e.g., HNC, CNO, amides, fullerenes/fulleranes, nanodiamonds, polycyclic aromatic hydrocarbons [PAHs], hydrogenated amorphous carbon [HACs], oxygen-bearing side groups on carbon rings [similar to those found in coal], iron oxides, and silicon disulphide and titanium carbide [TiC]; see Kwok, Volk, & Hrivnak 1989, 1999; Sourisseau et al. 1992; Webster 1995; Hill et al. 1998; Justtanont et al. 1996; Volk et al. 1999; Buss et al. 1990; Grishko et al. 2001; Papoular 2000; Cox 1990; Goebel 1993; von Helden et al. 2000).

Most of these species have since been discarded as carriers, with HACs/PAHs and TiC as the current most favored candidates. However, problems associated with these attributions suggest that other origins should be considered. These problems include: (1) in the spectra of HACs (Grishko et al. 2001), it is impossible to isolate the 21 μm feature; and (2) the spectrum of TiC gives a good match to both the shape and position of the observed feature; however, either unrealistically high mass-loss rates at the end of the AGB are needed to produce sufficient concentrations of TiC grains (M. Meixner et al. 2003, in preparation), or TiC must be an extremely

efficient UV/visible absorber and/or IR emitter (Hony et al. 2003; Chigai et al. 2003). Recent observations by Kwok, Volk, & Hrivnak (2002) show that the 21 μm feature does not seem to be associated with an extraordinarily high mass ejection phenomenon. Furthermore, only very small "nanoclusters" ($25 \rightarrow 127$ atoms) of TiC exhibit the 21 μm feature (von Helden et al. 2000). For larger grains, the feature is very weak, if seen at all, and is shifted to $\sim$19 μm (this paper; Kimura & Kaito 2003; Henning & Mutschke 2001). Another problem with the TiC hypothesis is the lack of supporting evidence in meteorites. Pristine samples of the circumstellar dust that formed around evolved stars can be found in meteorites in the guise of presolar grains (e.g., Bernatowicz 1997; Hoppe & Ott 1997 and references therein). Their anomalous isotopic compositions suggest that most of these grains form around AGB stars. Submicron-sized ($\sim$30–500 nm) TiC grains have been found inside micron-sized graphite grains (Stadermann et al. 2003; Bernatowicz et al. 1991, 1996). Therefore, TiC grains must form in AGB circumstellar environments. However, these grains are so large that they would not carry the 21 μm feature, and most of the available Ti must be incorporated into these "large" TiC grains.

Another presolar grain, which is much more abundant in meteorites, is silicon carbide (SiC). SiC is believed to be a significant constituent of the dust around C-rich AGB stars. Its well-known infrared (IR) peak at $\sim$11.3 μm is observed in many C star spectra (e.g., Speck, Barlow, & Skinner 1997). The complex spectral behavior of the many polymorphs of SiC has been the target of recent research (e.g., Speck, Hofmeister, & Barlow 1999; Hofmeister, Rosen, & Speck 2000; Papoular et al. 1998; Mutschke et al. 1999; Andersen et al. 1999; Devaty & Choyke 1997), and it is still revealing its secrets. This paper presents new laboratory data for SiC and shows that it has an IR peak that matches the observed 21 μm feature.

2. EXPERIMENTAL WORK

The α-SiC sample was obtained from Alpha/Aesar and is of the 6H polytype. The granular β-SiC sample (polytype 3C; average grain size of $\sim$1 μm) was donated by the Superior Graphite Company. A wafer of β-SiC (380 μm thick) made by chemical vapor deposition was purchased from the Rohm & Haas Company. TiC from Alpha/Aesar has an average grain size of 2 μm. These samples are at least 99.5% pure. The nanosample is mostly 3C, with a small and variable ($\sim$10%) amount of the 6H polytype, as determined by X-ray powder diffraction (XRD). XRD peak widths suggest particle sizes of 2–5 nm. The sample was produced through gas-phase combustion (Axelbaum et al. 1996) and consists of micron-sized clumps of the nanocrystals.

Thin films were produced by compression of the sample in a diamond anvil cell. From observation of relief in a binocular microscope, all film thicknesses are near 1 μm, roughly 10 times the thickness used in observing the fundamental IR mode (Speck, Hofmeister, & Barlow 1999). The cell serves as the sample holder and, when empty, as the reference. Far-infrared (650–10 cm^{-1}; 15–1000 μm) spectra at room temperature were obtained at 1 cm^{-1} resolution using an evacuated Bomem DA 3.02 Fourier transform interferometer with a liquid-helium–cooled Si bolometer. Weak derivative features occur in some spectra at 26.3, 22.7, and 19.8 μm; these are artifacts traceable to sharp peaks in the instrumental baseline, arising from the coating on the Mylar beam splitter. For procedural details, see Hofmeister (1995).

Reflectivity data were obtained from the wafer at normal incidence using a Spectra-Tech microscope for both the far-IR range (as above) and for the mid-IR (450–4000 cm^{-1}; 22-2 μm) with a KBr beam splitter and a HgCdTe detector. The data were merged, and a Kramers-Kronig analysis was run on the merged file. These results were used as the input to a damped harmonic oscillator model, which provided the absorption coefficient (e.g., Hofmeister, Keppe, & Speck 2003; A. K. Speck & A. M. Hofmeister 2003, in preparation). This result was benchmarked against independent measurements of the low-frequency dielectric constant and the index of refraction in the visible. As a further cross-check, the wafer was broken, and a small section was ground to a wedge with an average thickness of 25 μm. Absorption spectra collected from this section matched the calculation, confirming the accuracy of our model. Details will be presented in A. K. Speck & A. M. Hofmeister (2003, in preparation). We also collected mid-IR absorption spectra from the full thickness of the wafer at ambient and liquid nitrogen temperatures, using a cryostat of our own design.

3. RESULTS

The 21 μm feature is seen clearly in the nano-SiC spectra and appears weakly in the granular β-SiC spectra (Fig. 1). The wafer of β-SiC has a barely resolvable feature. This sample is a light brown color, rather than the dark gray of the granular sample or the black of the nanosample. Bulk TiC has a peak at $\sim$19 μm; although this is weak (Fig. 1), it is the main band.

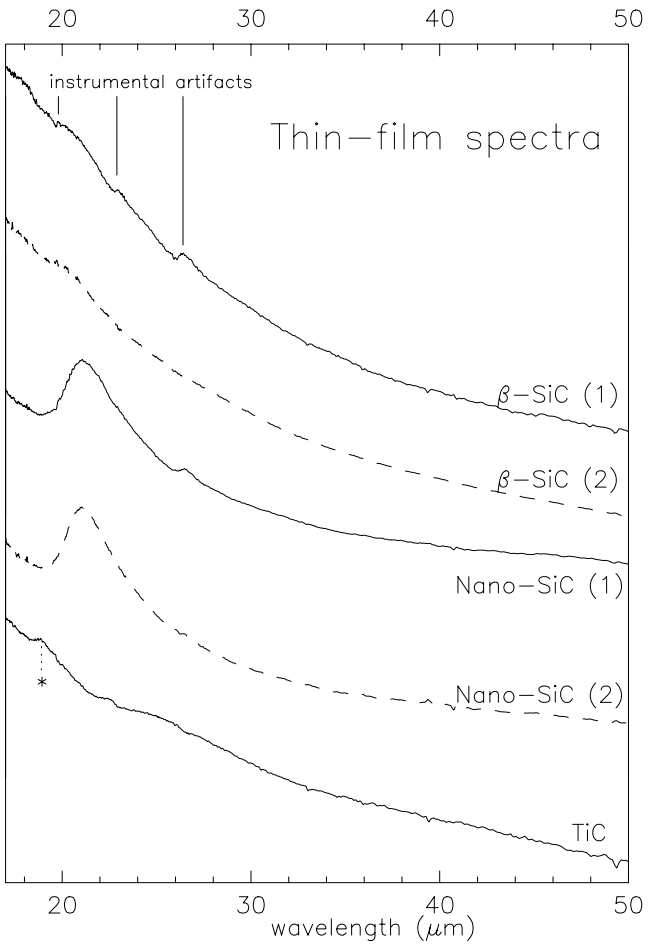

FIG. 1.—Far-IR spectra of SiC and TiC. Spectra were offset for clarity. The weak TiC feature at $\sim$19 μm is marked by an asterisk.

The 21 μm feature is not seen in the 6H α-SiC sample spectrum (not shown). The sloping baseline results from the intense band near 11 μm having sufficient breadth that it trails into the far-IR. Spectral subtraction of this slope allows the isolation of the 21 μm feature. The results (Fig. 2) recapitulate the isolated observed feature from the *Infrared Space Observatory* (*ISO*) data (Volk et al. 1999). The isolated β-SiC feature gives a good match to the peak position and shape of the observed feature. The spectrum of the nano-SiC sample also matches the shape, but the peak position is shifted to longer wavelengths by $\sim$1 μm. The difference between the two laboratory spectra is not due to stacking disorder because the Raman spectra of such samples exhibit broadening and distortion (Nakashima & Harima 1997). The effect on IR spectra should be analogous but is not observed here. The difference is therefore probably due to the mix of polytypes in the nanosample. This is consistent with the origin of the low-frequency peaks as folded acoustic modes in the cubic polytype (Choyke & Patrick 1962). The simplest stacking sequence (2H) folds the longitudinal acoustic (LA) mode at the zone edge of the cubic polymorph into the zone center at 16.3 μm; i.e., because the unit cell is doubled, the Brillouin zone is halved (Jones 1960). The existence of an "extra" band (i.e., one not predicted by symmetry) in the IR spectrum of β-SiC, as well as in the essentially cubic nanosample, is not unusual in that acoustic modes commonly appear in the IR through phonon-phonon interactions (e.g., Mitra 1969; Hofmeister & Mao 2001). The higher intensity in the nanosample is attributed to the small amount of the 6H polytype as revealed by XRD. The origin of the peak shift between the bulk and nanosamples is unclear, but shifts similar to those in Figure 1 are seen for the main IR bands of TiC and SiC (von Helden et al. 2000; Hofmeister, Rosen, & Speck 2000).

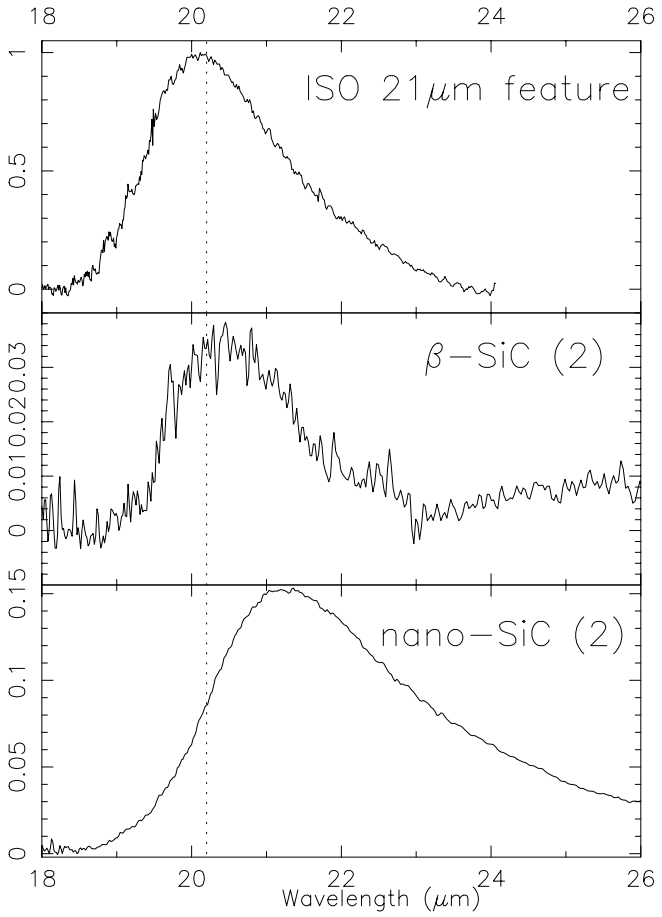

FIG. 2.—Isolated 21 μm feature from *ISO* spectra (*top*; see Volk et al. 1999), in the spectrum of β-SiC (*middle*), and in the spectrum of nano-SiC (*bottom*).

Alternatively, the feature may be connected with defects in the structure, such as extra C atoms in interstitial sites, or with clusters of C atoms or possibly of Si atoms within the structure. The latter hypothesis is consistent with intensity of the feature increasing from the wafer to the granular to the nano-SiC samples, which corresponds with the color becoming progressively darker. The 6H sample is paler than the wafer and lacks the feature. Moreover, pure SiC is colorless (e.g., synthetic moissanite used as a diamond substitute in jewelry), which further suggests that the colored samples likely have minute inclusions of graphite.

The hypothesis that the 21 μm feature is due to impurities in the SiC grains is supported by the work of Suttrop et al. (1992), who found that this feature appears in the spectra of nitrogen-doped SiC samples. The 21 μm feature seen in N-doped SiC is most intense at 80 K and weaker at both higher and lower temperatures (Suttrop et al. 1992). This is consistent with expected nebular conditions and explains the appearance of the 21 μm feature in a small number of objects in which the temperature conditions are most conducive. The cooling dust around the star allows the feature to be seen, but as the dust continues to cool, the feature will weaken and disappear. The 6H-SiC sample in Suttrop et al. (1992) has an additional peak at 513 cm^{-1} (19.4 μm) that is not evident in the astronomical data. This is consistent with the attribution of the astronomical feature with β-SiC.

Cooling SiC appreciably narrows but slightly decreases the wavelength of most Raman peaks from various polytypes (Nakashima & Harima 1997 and references therein). The transverse acoustic (TA) mode from IR spectra behaves similarly (Satoh et al. 1998). However, the LA modes near 20–25 μm in some polytypes show substantial dependence on temperature and defect content (Nakashima & Harima 1997). Our IR spectra at cryogenic temperatures from the wafer of β-SiC are almost identical to room-temperature spectra. Although only the shoulders of the main peak are resolved, the information is sufficient to establish that the peak shift from 300 to 77 K is almost nil, and therefore the room-temperature data represent SiC in space well. The very small temperature shifts are attributed to the stiffness of the Si-C bond. Therefore, the astronomical feature could be due to cold, 3C β-SiC grains with carbon impurities. The derived profiles of the 21 μm feature depend somewhat on the baselines chosen, as the 21 μm feature is on a shoulder of the main Si-C stretching band. However, this is inconsequential because the conditions in the astronomical environment differ from those in the laboratory. The laboratory data were taken at room temperature, which generally produces wider peaks (although the 6H does not seem affected). The peaks we see in three of our samples (nanomixed, beta, and nanobeta) and those seen by Suttrop et al. (1992) differ in position and slightly in width. The laboratory data presented here are from thin films, whereas the astronomical observational spectra are produced by a distribution of grain of different sizes. Therefore, the astronomical spectra should produce a broader feature. However, the astronomical environment is much cooler than room temperature, which would narrow the feature. The

differences in observational conditions between the dusty stars and the laboratory offset (compensate for each other) and hence the good agreement.

We have used the β-SiC sample to model the astronomical spectra (Fig. 3). For this case, the damped harmonic oscillator model provides the strength of the main band. The results of Figure 1 were sutured to this spectrum, assuming that the films are 10 μm thick. In actuality, the films are about 4 μm thick. Given that the feature depends on defects, and that the feature in the wafer was difficult to see for a 20 μm section, this thickness serves as a average value for our two samples of cubic SiC. This compromise may not represent dust in space, and it is possible that the feature is strong, as in our nanosample. The variable strength for this feature means that the ratio of the 11 and 21 μm peaks may not precisely fixed, unless conditions of formation are the same. The results (Fig. 3) show that the data are well represented by the SiC grains having sizes of 1 μm and temperatures near 50–60 K and with blackbody emissions of about 100–200 K. These blackbodies could be graphite, or iron particles, or large SiC grains or agglomerates of grains. The astronomical data can be fitted to larger or smaller grains or to a range of grain sizes with similar temperatures. The fit is not unique. However, low temperatures are needed to fit the weak 21 μm band and the strong 11 μm band simultaneously for sizes of the order of 1 μm and smaller and for the band strength assumed here. Higher temperatures are possible for very large grain sizes or for samples with intense 21 μm bands.

4. DISCUSSION

To better constrain the carrier of this enigmatic 21 μm feature we must consider the environment with which it is associated. What are the characteristics of PPNs that could contribute to the appearance of this feature? (1) As the circumstellar shell drifts away from the central star, the dust temperature decreases from $\sim$300–1000 to $\sim$50–150 K. (2) The expansion of the dust shell causes a decrease in the dust density. These dust shells are always optically thin. (3) There is the onset of the fast wind, a stellar wind with a velocity of $\sim$1000 km s^{-1}, which may result in energetic grain-grain collisions (e.g., Meixner et al. 1997; Jura & Kroto 1990).

The cooling of dust grains shifts the peak of the underlying continuum emission and thus suppresses features shortward of the continuum peak and favors features at around the peak wavelength (at $\sim$20 μm for a 150 K blackbody). In this way it is possible to see features that would be difficult to identify in the spectra of hotter grains. This is demonstrated in Figure 3, which shows the effects of multiplying the SiC emission spectra (derived from the absorption coefficient) by blackbody curves for 60 and 100 K. At 100 K, the band areas are nearly the same in the emission spectra, but at 60 K the 10 μm band is a small fraction of the 21 μm band. In Figure 3, this spectrum is compared to the observed *ISO* spectrum of IRAS 07134+1005 (from Hrivnak, Volk, & Kwok 2000) and shows a very good match, as well as the dominance of the 21 μm feature over the classic 11.3 μm SiC feature.

Fitting the object requires contributions from SiC with a range of temperatures, as well as some blackbody components, representing either very large SiC grains or an opaque substance such as graphite, amorphous carbon, or metallic iron. The fits shown are for grain sizes of 1 μm, but spectra of other grain sizes, or a range of grain sizes, also fit the spectra. Our fits do not account for scattering losses, which may be the reason for the model having excess intensity at long

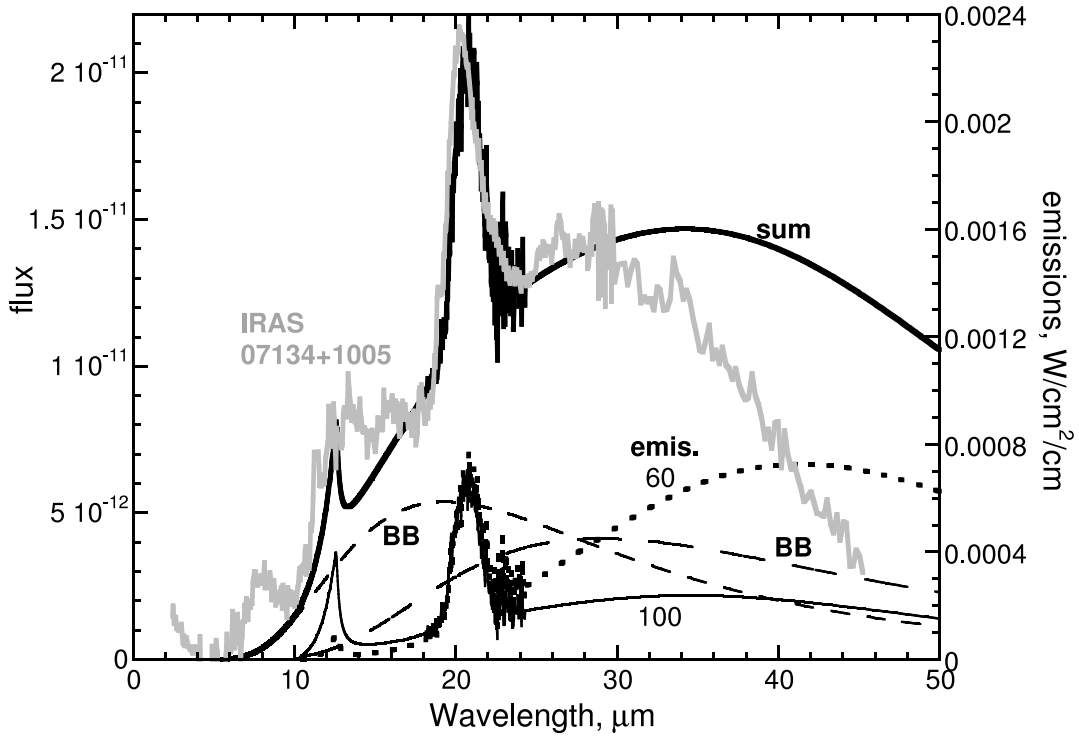

FIG. 3.—Comparison of IRAS 07134+1005 to emission spectra of β-SiC particles with an average diamper of 1 μm and blackbody curves. *Gray line*: *ISO* spectrum of IRAS 07134+1005 (Hrivnak, Volk, & Kwok 2000). *Thick solid line*: Sum of components. *Light lines*: Components of fitting. *Solid line*: Emissions of β-SiC at 100 K. *Dotted line*: Emissions of β-SiC at 60 K. *Short-dashed line*: Blackbody at 150 K. *Long-dashed line*: Blackbody at 100 K. The emissivity of SiC was calculated as described in the text. Flux for the *ISO* data is in units of W m^{-2}.

wavelengths. The broad bumps near 7 and 12 μm could be due to dust at higher temperatures ($\sim$225 and 400 K).

Kwok, Volk, & Hrivnak (2002) showed that the 21 μm feature is spatially coincident with emission in the 11.3 μm region and the underlying continuum. Both these bands will receive contributions from SiC. Moreover, during the PPN and PN phase there is an increase in PAH emission because of the increase in ultraviolet photons available to pump the emission. These emission features can bury the 11.3 μm SiC feature. Therefore, under these conditions, the 21 μm feature becomes much stronger and more easily observed than the 11.3 μm SiC feature. The relative strength of the 21 μm feature seems to be linked to the color of the sample, with the blacker samples having the strongest features. It is possible that the feature is due to carbon impurities in these grains (cf. A. P. Jones 2003, private communication).

With the onset of the PN phase, the central star emits high-energy photons that ionize the surrounding media and can destroy very small dust grains close to the central star (cf. Speck et al. 2002). Meanwhile, the dust shell continues to expand and thus cools and becomes less dense. The cooling of the dust grains alone is enough to suppress the 21 μm feature. Nano-SiC in the densest part of the dust shell closest to the star will be destroyed, and the outer part of the shell will have too low a density to produce an observable feature. Furthermore, Suttrop et al. (1992) showed that the 21 μm feature is strongest at $\sim$80 K and weakens at lower temperatures. Therefore, the best candidates for the carrier of the 21 μm feature are cool ($\sim$100 K) micron-sized β-SiC and nano-SiC grains with carbon impurities. The appearance of the 21 μm feature in two PN spectra (Hony, Waters, & Tielens 2001) suggests that the environment around PNs can produce this feature. This supports the attribution to micron-sized β-SiC grains, which could survive the onset of the ionizing radiation. In this scenario the emergence of the 21 μm feature is not due to the formation of a new dust species during the PPN phase, but rather that the physical conditions around AGB stars (and possibly PNs) conspire against the observation of this feature. During the PPN phase the combination of dust temperature, optical depth, and possibly grain processing in the fast wind provide optimal conditions for observing the 21 μm feature. However, the efficient dredge-up of *s*-process elements that has occurred in these stars (Van Winckel & Reyniers 2000) will also increase the carbon abundance. Therefore, the amount of carbon impurities in SiC should have increased with the evolution of the star. In this case, there is a small change in the nature of the dust grains that forms that would also increase the strength of the 21 μm feature.

Studies of meteoritic presolar SiC grains have yielded some interesting results regarding possible processing of these grains during the lifetime of a C-rich AGB star. Prombo et al. (1993) found a correlation between grain size and the enhancement of *s*-process elements in SiC grains in the Murchison meteorite such that the smallest grains have the highest concentrations of *s*-process elements and the larger grains are closer to solar isotopic composition. Similar results were found for SiC grains in the Indarch meteorite (Jennings et al. 2002). This implies that early in a C star's life, it produces larger grains. Later, as dredge-up enhances the concentration of *s*-process elements in the circumstellar shell, the grains are smaller, either through not growing to larger sizes or through the breakup of larger grains. This supports the idea of grain-grain collisions to produce a population of smaller grains formed at the very end of the mass-loss phase, when the *s*-process abundances are highest. All the 21 μm PPNs have high *s*-process abundances (Van Winckel & Reyniers 2000); therefore, we suggest that the 21 μm feature is due to the smaller, *s*-process–enriched grains with carbon impurities found around these objects.

Recent studies of many meteoritic grains showed that while large (>1 μm) presolar SiC grains are consistently of the β-polymorph, the smaller grains contain both α- and β-polymorphs (Daulton et al. 1998). However, the α-polymorph is of the simplest hexagonal 2H type and not the more common 6H type that results from the annealing of β-SiC grains (Daulton et al. 2002). Indeed, the formation temperature of 2H-SiC is lower than that of β-SiC, and therefore processing of β-SiC is unlikely to form this polymorph. The 2H-SiC has not yet been characterized spectroscopically. However, since only $\sim$10% of the meteoritic SiC is of the 2H polytype, it is unlikely that we will be able to resolve its contribution from that of the β-polymorph. It would be interesting to investigate the meteoritic presolar SiC grains with high *s*-process abundances to see whether they have higher carbon contents.

5. CONCLUSIONS

We have presented new laboratory data for SiC and shown that it has a spectral feature that is a good candidate for the carrier of the 21 μm feature. We suggest that cooling and processing of the SiC grains known to exist around C-rich AGB stars are responsible for the emergence of the enigmatic 21 μm feature.

We would like to thank Kevin Volk for access to his *ISO* spectra, and Tyrone Daulton and Christine Jennings for their input on meteoritic grains. Margaret Meixner is also thanked for purchasing the β-SiC wafer used in our experiments. A. M. H. was supported by NSF AST 98-05924.

REFERENCES

Andersen, A. C., Jäger, C., Mutschke, H., Braatz, A., Clément, D., Henning, Th., Jørgensen, U. G., & Ott, U. 1999, A&A, 343, 933
Axelbaum, R. L., Lottes, C. R., Rosen, L. J., & Huertes, J. I. 1996, in 26th Int. Symp. on Combustion (Pittsburgh: Combustion Inst.), A1891
Bernatowicz, T. 1997, in ASP Conf. Ser. 122, From Stardust to Planetesimals, ed. Y. J. Pendleton (San Francisco: ASP), 227
Bernatowicz, T. J., Amari, S., Zinner, E. K., & Lewis, R. S. 1991, ApJ, 373, L73
Bernatowicz, T. J., Cowsik, R., Gibbons, P. C., Lodders, K., Fegley, B., Amari, S., & Lewis, R. S. 1996, ApJ, 472, 760
Buss, R. H., Jr., et al. 1990, ApJ, 365, L23
Chigai, T., Yamamoto, T., Kaito, C., & Kimura, Y. 2003, ApJ, 587, 771
Choyke, W. J., & Patrick, L. 1962, Phys. Rev., 127, 1868
Cohen, M., Barlow, M. J., Liu, X.-W., & Jones, A. F. 2002, MNRAS, 332, 879
Cox, P. 1990, A&A, 236, L29
———. 1993, in ASP Conf. Ser. 41, Astronomical Infrared Spectroscopy: Future Observational Directions, ed. S. Kwok (San Francisco: ASP), 163
Daulton, T. L., Bernatowicz, T. J., Lewis, R. S., Messenger, S., Stadermann, F. J., & Amari, S. 2002, in 33rd Annual Lunar and Planetary Science Conf. (Houston: Lunar and Planetary Inst.), A1127
Daulton, T. L., Lewis, R. S., & Amari, S. 1998, Meteoritics Planet. Sci., 32, A37
Devaty, R. P., & Choyke, W. J. 1997, Phys. Status Solidi A, 162, 5
Goebel, J. H. 1993, A&A, 278, 226
Grishko, V. I., Tereszchuk, K., Duley, W. W., & Bernath, P. 2001, ApJ, 558, L129

Henning, T., & Mutschke, H. 2001, Spectrochim. Acta A, 57, 815
Hill, H. G. M., Jones, A. P., & D'Hendecourt, L. B. 1998, A&A, 336, 41
Hofmeister, A. M. 1995, in Practical Guide to Infrared Microspectroscopy, ed. H. Humicki (New York: Marcel Dekker, Inc.), 377
Hofmeister, A. M., Keppel, E., & Speck, A. K. 2003, MNRAS, 345, 16
Hofmeister, A. M., & Mao, H. K. 2001, Amer. Mineral., 86, 622
Hofmeister, A. M., Rosen, L. J., & Speck, A. K. 2000, in ASP Conf. Ser. 196, Thermal Emission Spectroscopy and Analysis of Dust, Disks, and Regoliths, ed. M. L. Sitko, A. L. Sprague, & D. K. Lynch (San Francisco: ASP), 291
Hony, S., Tielens, A. G. G. M., Waters, L. B. F. M., & de Koter, A. 2003, A&A, 402, 211
Hony, S., Waters, L. B. F. M., & Tielens, A. G. G. M. 2001, A&A, 378, L41
Hoppe, P., & Ott, U. 1997, in Astrophysical Implications of the Laboratory Study of Presolar Materials, ed. T. Bernatowicz & E. Zinner (New York: AIP), 27
Hrivnak, B. J., Volk, K., & Kwok, S. 2000, ApJ, 535, 275
Iben, I., Jr., & Renzini, A. 1983, ARA&A, 21, 271
Jennings, C. L., Savina, M. R., Messenger, S., Amari, S., Nichols, R. H., Pellin, M. J., & Podosek, F. A. 2002, in 33rd Annual Lunar and Planetary Science Conf. (Houston: Lunar and Planetary Inst.), A1833
Jones, H. 1960, The Theory of Brillouin Zones and Electronic States in Crystals (Amsterdam: North Holland)
Jura, M., & Kroto, H. 1990, ApJ, 351, 222
Justtanont, K., Barlow, M. J., Skinner, C. J., Roche, P. F., Aitken, D. K., & Smith, C. H. 1996, A&A, 309, 612
Kimura, Y., & Kaito, C. 2003, MNRAS, in press
Kwok, S., Volk, K., & Hrivnak, B. J. 1989, ApJ, 345, L51
———. 1999, in IAU Symp. 191, Asymptotic Giant Branch Stars, ed. T. Le Bertre, A. Lèbre, & C. Waelkens (San Francisco: ASP), 297
———. 2002, ApJ, 573, 720
Meixner, M., Skinner, C. J., Graham, J. R., Keto, E., Jernigan, J. G., & Arens, J. F. 1997, ApJ, 482, 897
Mitra, S. S. 1969, in Optical Properties of Solids, ed. S. Nudelman & S. S. Mitra (New York: Plenum), 333
Mutschke, H., Andersen, A. C., Clément, D., Henning, Th., & Peiter, G. 1999, A&A, 345, 187
Nakashima, S., & Harima, H. 1997, Phys. Status Solidi A, 162, 39
Omont, A., et al. 1995, ApJ, 454, 819
Papoular, R. 2000, A&A, 362, L9
Papoular, R., Cauchetier, M., Begin, S., & Lecaer, G. 1998, A&A, 329, 1035
Prombo, C. A., Podosek, F. A., Amari, S., & Lewis, R. S. 1993, ApJ, 410, 393
Satoh, K., Harada, Y., Nakata, H., & Ohyama, T. 1998, Mater. Sci. Engineering, B56, 72
Sourisseau, C., Coddens, G., & Papoular, R. 1992, A&A, 254, L1
Speck, A. K., Barlow, M. J., & Skinner, C. J. 1997, MNRAS, 288, 431
Speck, A. K., Hofmeister, A. M., & Barlow, M. J. 1999, ApJ, 513, L87
Speck, A. K., Meixner, M., Fong, D., McCullough, P. R., Moser, D., & Ueta, T. 2002, AJ, 123, 346
Stadermann, F. J., Bernatowicz, T., Croat, T. K., Zinner, E., Messenger, S., & Amari, S. 2003, in 34th Annual Lunar and Planetary Science Conf. (Houston: Lunar and Planetary Inst.), A1627
Suttrop, W., Pensi, G., & Choyke, W. J. 1992, J. Appl. Phys., 72, 3708
Van Winckel, H., & Reyniers, M. 2000, A&A, 354, 135
Volk, K., Kwok, S., & Hrivnak, B. J. 1999, ApJ, 516, L99
Volk, K., et al. 2003, in IAU Symp. 209, Planetary Nebulae: Their Evolution and Role in the Universe, ed. S. Kwok, M. Dopita, & R. Sutherland (San Francisco: ASP), in press
von Helden, G., Tielens, A. G. G. M., van Heijnsbergen, D., Duncan, M. A., Hony, S., Waters, L. B. F. M., & Meijer, G. 2000, Science, 288, 313
Webster, A. 1995, MNRAS, 277, 1555